

# Crossed Molecular Beam Study on the Reaction of Boron Atoms, $B(^2P_j)$ , with Allene, $H_2CCCH_2(X^1A_1)$

Fangtong Zhang,<sup>†</sup> Hui Lun Sun,<sup>‡</sup> Agnes H. H. Chang,<sup>‡</sup> Xibin Gu,<sup>†</sup> and Ralf I. Kaiser<sup>\*,†</sup>

Department of Chemistry, University of Hawaii, Honolulu, Hawaii 96822, and Department of Chemistry, National Dong Hwa University, Hualien 974, Taiwan

Received: August 7, 2007; In Final Form: October 2, 2007

The reaction of ground state boron atoms,  $^{11}B(^2P_j)$ , with allene,  $H_2CCCH_2(X^1A_1)$ , was studied under single collision conditions at a collision energy of 21.5 kJ mol<sup>-1</sup> utilizing the crossed molecular beam technique; the experimental data were combined with electronic structure calculations on the  $^{11}B_3H_4$  potential energy surface. The chemical dynamics were found to be indirect and initiated by an addition of the boron atom to the  $\pi$ -electron density of the allene molecule leading ultimately to a cyclic reaction intermediate. The latter underwent ring-opening to yield an acyclic intermediate  $H_2CCBCH_2$ . As derived from the center-of-mass functions, this structure was long-lived with respect to its rotational period and decomposed via an atomic hydrogen loss through a tight exit transition state to form the closed shell,  $C_{2v}$  symmetric  $H-C\equiv C-B=CH_2$  molecule. A brief comparison of the product isomers formed in the reaction of boron atoms with methylacetylene is also presented.

## 1. Introduction

In recent years, the chemistry of boron has received special attention due to its vast application potentials in combustion systems,<sup>1–3</sup> semiconductor manufacturing,<sup>4–6</sup> nanotubes,<sup>7–9</sup> and organoboron synthesis.<sup>10–12</sup> In an effort to pursue systematically the mechanisms involved in the boron combustion chemistry, elementary reactions of boron atoms with unsaturated hydrocarbons were widely studied both experimentally and theoretically.<sup>13–19</sup> In recent years, crossed molecular beams have been utilized to unravel the reaction dynamics of these elementary reactions under collision-free conditions in the gas phase on the molecular level.<sup>19–25</sup> To date, acetylene,<sup>19,21,24</sup> ethylene,<sup>20</sup> and benzene<sup>22,25</sup> have been chosen as prototype reaction partners carrying carbon–carbon triple and double bonds as well as an “aromatic” system. In addition, the influence of the structure of distinct isomers on the reaction dynamics has always been a fascinating topic and attracted considerable attention. Here, methylacetylene ( $CH_3CCH$ ) and allene ( $H_2CCCH_2$ ) present a unique isomer pair to be investigated via their chemical reaction dynamics and kinetics.<sup>26–32</sup> For instance, Farrell et al. measured the hydrogen chloride (HCl) production for atomic chlorine reactions with both  $C_3H_4$  isomers.<sup>28,33</sup> They found that the reaction of chlorine atoms with allene is dominated at low temperature by addition and driven by formation of the resonantly stabilized chloroallyl radical. The formation of HCl, which accounts for only 2% of the reactivity at 292 K, increased with temperature and was determined to be the dominant pathway at temperatures larger than 800 K. However, in the case of its reaction with methylacetylene, in the temperature range 292–400 K the reaction proceeded via both abstraction and addition–elimination pathways. At  $T > 500$  K, abstraction constituted the major reactive pathway. This is a perfect example demonstrating the steric effects, electronic structure, and distinct cone of acceptances on a chemical reaction. Various

systems were also investigated utilizing the crossed molecular beam (CMB) approach.<sup>26,34–39</sup> Balucani et al. studied the gas-phase reaction of the cyano radical,  $CN(X^2\Sigma^+)$ , with methylacetylene and allene.<sup>34,35,37,40</sup> Kaiser et al. investigated the reactions of carbon  $C(^3P_j)$ <sup>38,41</sup> and of  $C_2(X^1\Sigma_g^+/a^3\Pi_u)$ <sup>42,43</sup> with both isomers to unravel the isomer-specific reaction products. Here, we expand these studies to the reaction of atomic boron,  $B(^2P)$ , with allene and compare these findings to the  $B(^2P)/CD_3CCH$ <sup>44</sup> and  $C(^3P_j)/C_3H_4$  systems investigated previously.<sup>38,41</sup>

## 2. Experimental and Data Analysis

The elementary reactions of ground state boron atoms,  $B(^2P_j)$ , with allene,  $H_2CCCH_2(X^1A_1)$ , were conducted in a universal crossed molecular beams machine under single collision conditions at the University of Hawaii.<sup>45–47</sup> A pulsed boron atom beam was generated in the primary source chamber by laser ablation of a boron rod at 266 nm (30 Hz; 5–10 mJ per pulse).<sup>48</sup> The ablated species were seeded in neat carrier gas (helium, 99.9999%, Airgas) released by a Proch-Trickl pulsed valve at 4 atm backing pressure. After passing a skimmer, a four-slot chopper wheel selected a part of the boron beam at a peak velocity,  $v_p$ , of  $2070 \pm 10$  ms<sup>-1</sup>; a speed ratio of  $3.4 \pm 0.2$  was obtained. Note that the ablation beam contains both  $^{11}B$ (80%) and  $^{10}B$ (20%) species in their nature abundances. The experimental conditions such as the delay times between the laser and the pulsed valve as well as the laser power and laser focus were optimized so that neither metastable nor electronically excited boron atoms existed in the beam. Therefore, a chopper wheel is crucial to eliminate contributions of electrically excited/metastable boron atoms which are present in the fast part of the unchopped ablation beam.<sup>49</sup> The segment of the boron beam crossed a pulsed allene beam ( $H_2CCCH_2$ , 98%, Sigma-Aldrich; 550 Torr) released by a second pulsed valve perpendicularly in the interaction region. This segment of the beam crossed had a peak velocity of  $840 \pm 3$  ms<sup>-1</sup> and a speed ratio of  $9.0 \pm 1.0$ . This resulted in a collision energy of  $21.5 \pm 0.2$  kJ mol<sup>-1</sup> for the  $^{11}B(^2P_j)/H_2CCCH_2$  system. The reactively scattered species

<sup>†</sup> University of Hawaii.

<sup>‡</sup> National Dong Hwa University.

were monitored using a quadrupole mass spectrometric detector in the time-of-flight (TOF) mode after electron-impact ionization of the molecules at 90 eV. This detector could be rotated within the plane defined by the primary and the secondary reactant beams to allow taking angular resolved TOF spectra. At each angle, up to 300 000 TOF spectra were accumulated to obtain good signal-to-noise ratios. The recorded TOF spectra were then integrated and normalized to extract the product angular distribution in the laboratory frame (LAB). To collect information on the scattering dynamics, the laboratory data were transformed into the center-of-mass reference frame utilizing a forward-convolution routine.<sup>50,51</sup> This iterative method initially guessed the angular flux distribution,  $T(\theta)$ , and the translational energy flux distribution,  $P(E_T)$  in the center-of-mass system (CM). Laboratory TOF spectra and the laboratory angular distributions (LAB) were then calculated from the  $T(\theta)$  and  $P(E_T)$  function and averaged over a grid of Newton diagrams accounting for the velocity and angular spread of each beam and the detector acceptance angle. Best fits were obtained by iteratively refining the adjustable parameters in the center-of-mass functions.

### 3. Results

**3.1. Laboratory Data.** In the reaction of  $^{11}\text{B}(^2\text{P}_j)$  with allene,  $\text{H}_2\text{CCCH}_2(\text{X}^1\text{A}_1)$ , reactive scattering signal was monitored in the range of mass-to-charge ratios,  $m/z$ , from 50 to 46. At each angle, the TOFs of these ions were, after scaling, superimposable, indicating that signal at lower  $m/z$  ratios originates from dissociative ionization of the parent molecules in the electron impact ionizer. This finding alone implies that the boron versus hydrogen atom exchange pathway is open; no molecular hydrogen loss could be observed. The signal at  $m/z = 50$  originated therefore from  $^{11}\text{BC}_3\text{H}_3^+$ , at  $m/z = 49$  from  $^{11}\text{BC}_3\text{H}_2^+$  and  $^{10}\text{BC}_3\text{H}_3^+$ ,  $m/z = 48$  from  $^{11}\text{BC}_3\text{H}^+$  and  $^{10}\text{BC}_3\text{H}_2^+$ ,  $m/z = 47$  from  $^{11}\text{BC}_3^+$  and  $^{10}\text{BC}_3\text{H}^+$ , and  $m/z = 46$  from  $^{10}\text{BC}_3^+$ . It is interesting to discuss briefly the influence of the  $^{10}\text{B}$  isotope on the shape of the TOF spectra at  $m/z$  lower than 50. Considering the center of mass angles of the  $^{11}\text{B}(^2\text{P}_j)$ -allene and  $^{10}\text{B}(^2\text{P}_j)$ -allene systems of  $55.9^\circ$  and  $58.4^\circ$ , we would expect an offset of the laboratory angular distributions of  $m/z = 50$  originating from  $^{11}\text{BC}_3\text{H}_3^+$  and  $m/z = 49$  from  $^{11}\text{BC}_3\text{H}_2^+$  and  $^{10}\text{BC}_3\text{H}_3^+$  by about  $2.5^\circ$ . This offset has been observed recently in the weakly exoergic reaction of  $^{11}\text{B}(^2\text{P}_j)/^{10}\text{B}(^2\text{P}_j)$  with acetylene.<sup>52</sup> However, the strongly exoergic nature of the present reaction combined with the velocity and angular spreads of the boron atom beam of  $2.8^\circ$  wash out this offset in the boron-allene system. We would like to stress that no radiative association to  $\text{BC}_3\text{H}_4^+$  ( $m/z = 51$ ) or higher masses were detected. Consequently, TOF data were taken at  $m/z = 50$  because of the highest signal-to-noise ratio at this mass-to-charge ratio (Figure 1). The corresponding LAB distribution is shown in Figure 2. Note that the laboratory angular distribution of the heavy reaction product of the generic formula  $^{11}\text{BC}_3\text{H}_3$  is forward-backward symmetric, peaks around  $55^\circ$  close to the center-of-mass angle  $55.9 \pm 0.3^\circ$  of the  $^{11}\text{B}(^2\text{P}_j)/\text{H}_2\text{CCCH}_2$  system, and is spread at least  $45^\circ$  within the scattering plane. This shape of the LAB distribution indicates that the reaction proceeds via indirect scattering dynamics involving  $^{11}\text{BC}_3\text{H}_4$  intermediate(s). It should be noted that the hydrogen abstraction channel to form the BH molecule plus the propargyl radical is too endoergic ( $+37 \text{ kJ mol}^{-1}$ ) to be open at our collision energy of  $21.5 \text{ kJ mol}^{-1}$ .

**3.2. Center-of-Mass Functions.** The corresponding center-of-mass translational energy distribution,  $P(E_T)$ , together with center-of-mass angular distribution,  $T(\theta)$ , for the title reaction

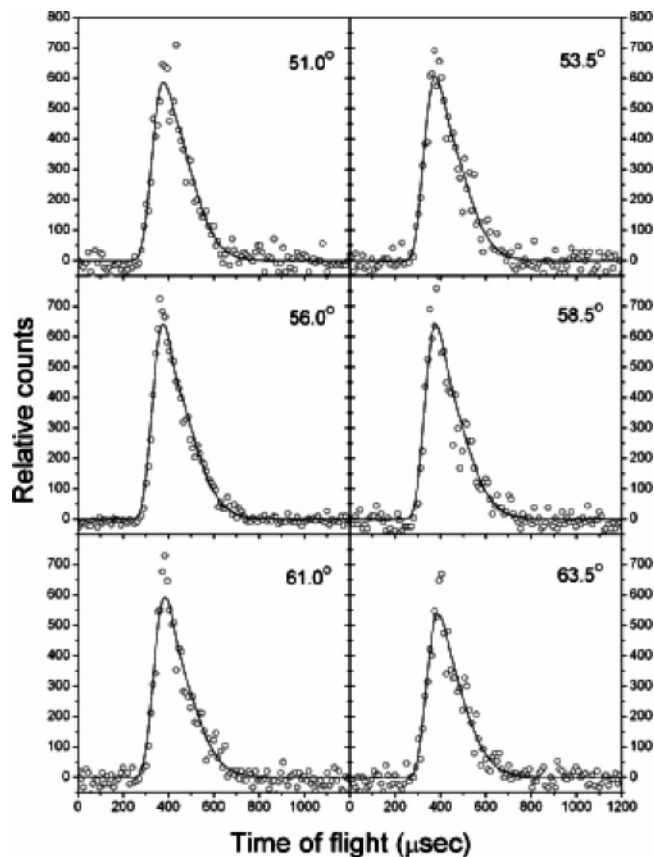


**Figure 1.** Time-of-flight data recorded at  $m/z = 50$  ( $^{11}\text{BC}_3\text{H}_3^+$ ) for selected laboratory angles at a collision energy of  $21.5 \text{ kJ mol}^{-1}$ . The circles represent the experimental data, and the solid lines, the fit. Each TOF spectrum has been normalized to the relative intensity of each angle.

to form  $^{11}\text{BC}_3\text{H}_3$  and atomic hydrogen are displayed in Figure 3. It is most noticeable that the best fits of the LAB distribution and the TOF data could be achieved with a single channel. The  $P(E_T)$  extends to a maximum translational energy release ( $E_{\text{max}}$ ) of  $155 \pm 5 \text{ kJ mol}^{-1}$ . Because a light hydrogen atom is emitted, this high-energy cutoff is relatively insensitive; adding or cutting up to  $10 \text{ kJ mol}^{-1}$  does not change the fit. It should be stressed that  $E_{\text{max}}$  is the absolute of the reaction exoergicity plus the collision energy. Therefore, by subtracting the collision energy ( $21.5 \text{ kJ mol}^{-1}$ ) from the high-energy cutoff, we are left with experimental exoergicity of  $134 \pm 15 \text{ kJ mol}^{-1}$ . This value can be utilized later to be compared with *ab initio* calculations to identify the structural isomer(s) formed. Second, the  $P(E_T)$  was found to peak away from zero translational energy at  $30\text{--}40 \text{ kJ mol}^{-1}$ ; this pattern likely indicates the existence of a tight exit transition state and hence a repulsive energy loss in the atomic hydrogen pathway from the decomposing  $^{11}\text{BC}_3\text{H}_4$  intermediate. Finally, the average amount of energy channeling into the translational degrees of freedom of the reaction products was calculated to be  $35 \pm 2\%$ .

We would like to discuss now the center-of-mass angular distribution. Best fits were achieved with distributions symmetric around  $90^\circ$ . This finding implies that the lifetime of the decomposing complex(es) is (are) longer than the (ir) rotational period. It should be emphasized that within the uncertainties of the experiment, the hydrogen loss pathway could be fit with either an isotropic or center-of-mass angular distribution holding a small maximum at  $90^\circ$ . Despite these uncertainties, the results indicate indirect scattering dynamics via the formation of  $^{11}\text{BC}_3\text{H}_4$  reaction intermediate(s). Also, the relatively moderate

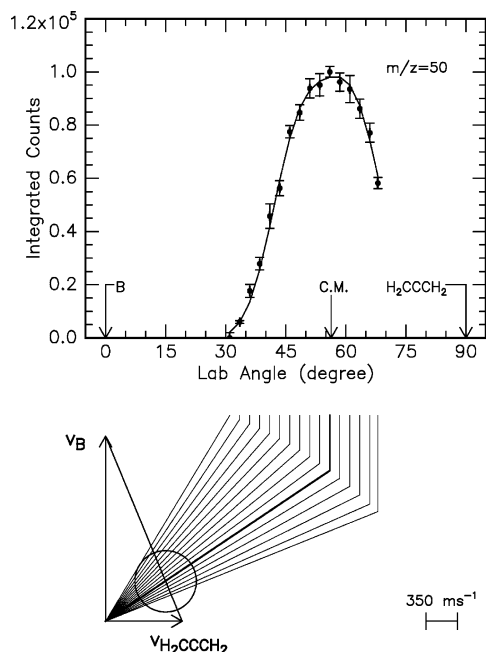


**Figure 2.** Lower: Newton diagram for the reaction of  $^{11}\text{B}(^2P_j)$  with  $\text{H}_2\text{CCCH}_2(X^1A_1)$  at a collision energy of  $21.5 \text{ kJ mol}^{-1}$ . The circle shows the maximum center-of-mass recoil velocity of the thermodynamically most stable  $^{11}\text{BC}_3\text{H}_3$  isomer ( $\text{H}-\text{C}\equiv\text{C}-\text{B}=\text{CH}_2$ ) assuming that no energy channels into the internal degrees of freedom. Upper: laboratory angular distribution of the  $^{11}\text{BC}_3\text{H}_3$  product at  $m/z = 50$ . Circles and  $1\sigma$  error bars indicate the experimental data; the solid line, the calculated distribution. The center-of-mass angle is indicated by C.M. The solid lines originating in the Newton diagram point to distinct laboratory angles whose TOF spectra are shown in Figure 1.

polarization of the  $T(\theta)$  can be understood in terms of total angular momentum conservation.<sup>53</sup> Here, most of the initial orbital angular momentum channels into the rotational excitation of the reaction products; this leads to a poor coupling between the initial and final orbital angular momenta.

#### 4. Discussion

To elucidate the reaction mechanism(s), it is important to clarify first the nature of the reaction product(s). Here, we compare the experimentally determined reaction energy of  $134 \pm 15 \text{ kJ mol}^{-1}$  with those obtained for different  $^{11}\text{BC}_3\text{H}_3$  isomers determined from *ab initio* electronic structure calculations. To compute relative energies of the  $^{11}\text{BC}_3\text{H}_3 + \text{H}$  products with respect to the atomic boron plus allene reactants, the hybrid density functional theory, the unrestricted B3LYP<sup>54,55</sup>/6-311G-(d,p)<sup>56,57</sup> was employed to obtain optimized geometries, harmonic frequencies, and the energies are further refined with the coupled cluster<sup>58–61</sup> CCSD(T)/cc-pVTZ with B3LYP/6-311G-(d,p) zero point energy corrections. The GAUSSIAN 98<sup>62</sup> and 03<sup>63</sup> program packages were utilized for the calculations. The geometrical structures of energetically accessible  $^{11}\text{BC}_3\text{H}_3$  isomers are compiled in Figure 4 together with the reaction energies, point groups, and ground state electronic wave functions. A comparison of the experimental reaction energy ( $-134 \pm 15 \text{ kJ mol}^{-1}$ ) with these computed values suggests that at least the thermodynamically most stable isomer, **p1** ( $\text{H}-\text{C}\equiv\text{C}-\text{B}=\text{CH}_2$ ) is formed ( $-131 \pm 10 \text{ kJ mol}^{-1}$ ). We acknowledge that at the present stage, we cannot provide quantitative information on the relative contribution of the thermodynamically less favorable isomers **p2–p4**.

We are combining now the assignment of the **p1** + H product channel with the information derived from the center-of-mass

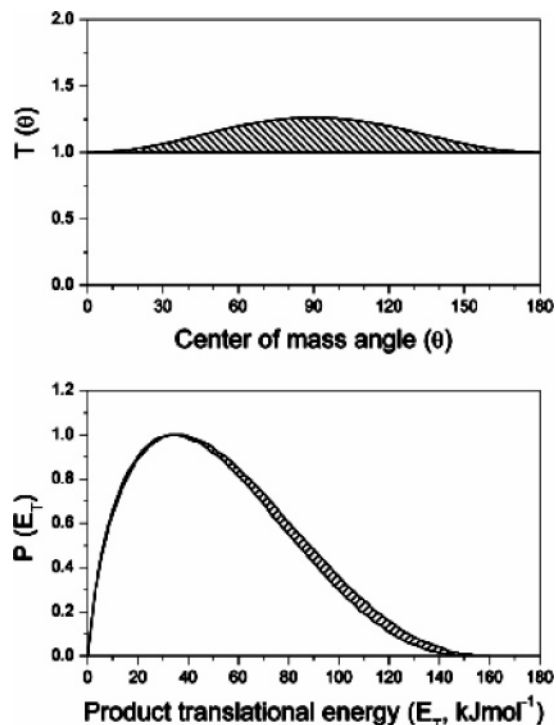


**Figure 3.** Lower: center-of-mass translational energy flux distribution for the reaction  $^{11}\text{B}(^2P_j) + \text{H}_2\text{CCCH}_2(X^1A_1) \rightarrow ^{11}\text{BC}_3\text{H}_3 + \text{H}$  at a collision energy of  $21.5 \text{ kJ mol}^{-1}$ . The two lines limit the range of acceptable fits to within  $1\sigma$  error bars. Upper: center-of-mass angular flux distribution for the reaction  $\text{B}(^2P_j) + \text{H}_2\text{CCCH}_2(X^1A_1) \rightarrow ^{11}\text{BC}_3\text{H}_3 + \text{H}$  at a collision energy of  $21.5 \text{ kJ mol}^{-1}$ . The two lines limit the range of acceptable fits within  $1\sigma$  error bars.

functions in an attempt to predict the underlying reaction mechanism. First, we have to compare the structure of the **p1** reaction product with the geometry of the atomic boron and allene reactant (Figure 5). In allene, the hydrogen atoms are connected pairwise to the terminal carbon atoms. Therefore, to correlate **p1** with allene, it is likely that in the reversed reaction of the hydrogen atom with **p1** ( $\text{H}-\text{C}\equiv\text{C}-\text{B}=\text{CH}_2$ ), atomic hydrogen adds to the terminal, acetylene carbon atom. Because **p1** is a closed shell molecule, this addition process should have an entrance barrier and hence a tight transition state similar to the reaction of atomic hydrogen with alkynes where typical entrance barrier are on the order of  $12\text{--}22 \text{ kJ mol}^{-1}$ .<sup>64</sup> This process would lead to an acyclic  $\text{H}_2\text{CCBCH}_2$  intermediate in which the boron atom is *formally* inserted between two carbon atoms of the allene molecule. This structure may be formed via an initial addition of atomic boron to one of the two carbon-carbon double bond of allene yielding a cyclic intermediate which can undergo ring opening to  $\text{H}_2\text{CCBCH}_2$ .

Having proposed this reaction mechanism, we are investigating now if this reaction sequence can be supported by electronic structure calculations (Figures 5 and 6). As a matter of fact, we found three barrierless entrance channels in the reaction of atomic boron with allene: (i) an addition to the terminal carbon atom, (ii) an addition to the central carbon atom, and (iii) an addition to one of the  $\text{C}=\text{C}$  bonds of allene leading to intermediated **i1**, **i2**, and **i3**. Both acyclic structures were found to isomerize easily to **i3**. Consequently, the cyclic structure **i3** presents the central reaction intermediate as proposed. A successive ring opening via a barrier of only  $13 \text{ kJ mol}^{-1}$  converts **i3** into **i4**. The latter was found to lose a hydrogen atom via a tight transition state located  $14 \text{ kJ mol}^{-1}$  above the separated products **p1** + H. Consequently, our proposed reaction mechanism could be verified computationally. This reaction

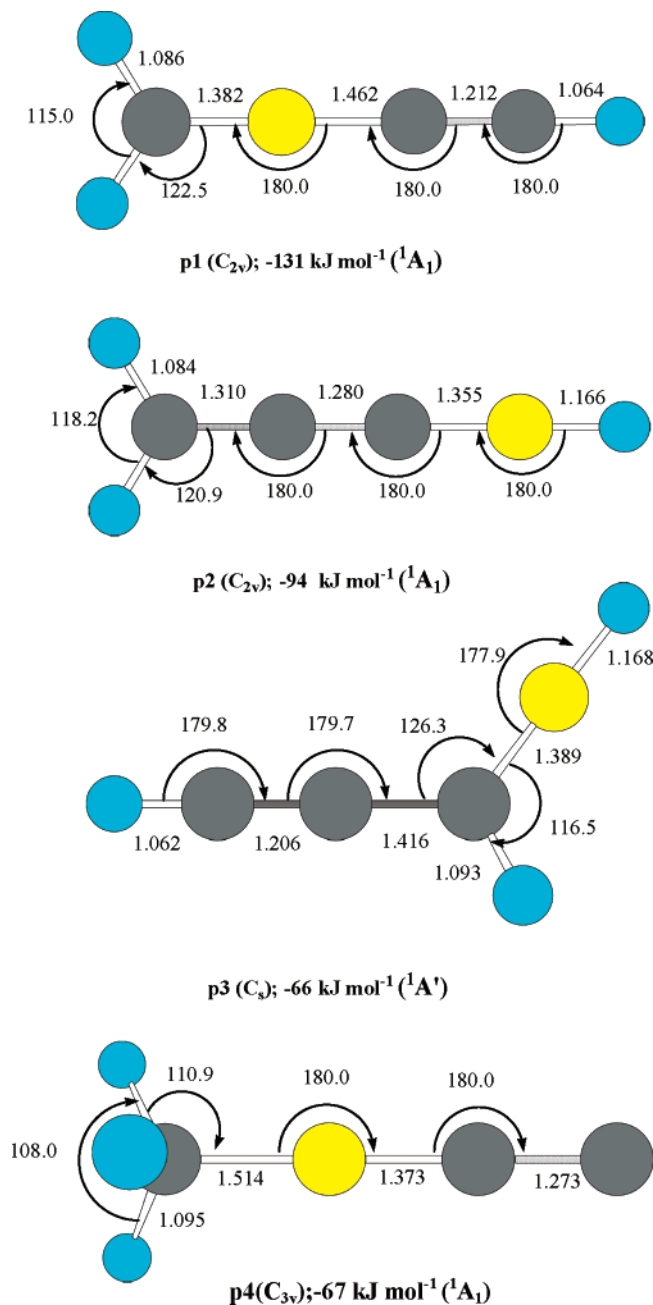


**Figure 4.** Structures of energetically accessible  $^{11}\text{BC}_3\text{H}_3$  isomers. Bond angles and lengths are given in degrees and angstroms, respectively. Point groups are given in parentheses. The energetics given present the exoergicities of the  $^{11}\text{BC}_3\text{H}_3 + \text{H}$  channel with respect to the separated atomic boron and allene reactants, respectively (key: yellow, boron; blue, hydrogen; black, carbon).

mechanism is also well supported by the indirect dynamics, as derived from the center-of-mass angular distribution (Figure 3). Based on the shape of the  $T(\theta)$ , the lifetime of the decomposing intermediate, here **i4**, is longer than its rotational period. Also, the average amount of energy channeling into the translational degrees of freedom of the reaction products of  $35 \pm 2\%$  is consistent with rather indirect scattering dynamics. Also, the tight exit transition state as verified in the computational study correlates nicely with the off-zero peaking of the center-of-mass translational energy distribution.

Finally, we comment briefly on the experimentally derived the forward-backward symmetric shape of the center-of-mass angular distribution. The reaction of boron atoms with allene depicts a long-established system in which the initial orbital

angular momentum  $\mathbf{L}$  is transformed mainly into the rotational excitation  $\mathbf{j}'$  of the polyatomic reaction products. Here, the total angular momentum  $\mathbf{J}$  is determined by eq 1 with the rotational angular momenta of the reactants and products  $\mathbf{j}$  and  $\mathbf{j}'$  and the initial and final orbital angular momenta  $\mathbf{L}$  and  $\mathbf{L}'$ .<sup>53</sup>

$$\mathbf{J} = \mathbf{L} + \mathbf{j} = \mathbf{L}' + \mathbf{j}' \quad (1)$$

Because the reactant beams are prepared in a supersonic expansion, the rotational excitation of the reactant molecules is expected to be small and eq 1 can be modified to

$$\mathbf{J} \approx \mathbf{L} = \mathbf{L}' + \mathbf{j}' \quad (2)$$

Because our electronic structure calculations suggest that the reaction of atomic boron with allene is barrierless and, hence, advances within orbiting limits, the maximum impact parameter  $b_{\text{max}}$  leading to the initial complex formation can be approximated in terms of the classical capture theory to be about  $3.2 \pm 0.2 \text{ \AA}$ . Because the maximum orbital angular momentum  $L_{\text{max}}$  relates to  $b_{\text{max}}$  via

$$L_{\text{max}} = \mu b_{\text{max}} v_r \quad (3)$$

where  $\mu$  is the reduced mass and  $v_r$  is the relative velocity of the reactants, this yields  $L_{\text{max}}$  values of  $120 \pm 10 \hbar$ . An upper limit of  $L'$  can also be estimated by assuming a relative velocity of the recoiling products corresponding to the average translational energy release  $\langle E_T \rangle$ , and choosing an allenic carbon-carbon double bond length of about  $1.4 \text{ \AA}$  as the exit impact parameter. This calculates  $L'$  to be on the order of  $25 \pm 10 \hbar$ . This visualizes that the initial orbital angular momentum is much larger than the final orbital angular momentum, and most of the initial orbital angular momentum channels into rotational excitation of the polyatomic product resulting into relatively weakly polarized  $T(\theta)$ . This weak  $\mathbf{L}-\mathbf{L}'$  correlation is a direct result of large impact parameters contributing to the complex formation and the inability of the departing hydrogen atom to carry significant orbital angular momentum.

## 5. Conclusions

The reaction of ground state boron atoms,  $^{11}\text{B}(^2\text{P}_1)$ , with allene,  $\text{H}_2\text{CCCH}_2(X^1A_1)$ , was studied under single collision conditions exploiting the crossed molecular beam technique and combining the experimental data with electronic structure calculations. The reaction dynamics were found to be indirect and initiated by an addition of the boron atom to the  $\pi$ -electron density of the allene molecule leading ultimately to a cyclic reaction intermediate **i3**. The latter, which is stabilized by  $208 \text{ kJ mol}^{-1}$  with respect to the separated reactants, undergoes ring-opening to yield an acyclic intermediate  $\text{H}_2\text{CCBCH}_2$  (**i4**). This structure was found to be long-lived with respect to its rotational period and decomposed via an atomic hydrogen loss through a tight exit transition state to the closed shell,  $C_{2v}$  symmetric molecule  $\text{H}-\text{C}\equiv\text{C}-\text{B}=\text{CH}_2$  (**p1**). The dynamics are very similar to the related reaction of ground state carbon atoms with allene investigated earlier. Both the carbon and boron atom add without entrance barrier to the  $\pi$ -electron density of the allene species resulting finally in cyclic reaction intermediates stabilized by  $200\text{--}270 \text{ kJ mol}^{-1}$  with respect to the reactants. These intermediates ring open via barriers of  $10\text{--}40 \text{ kJ mol}^{-1}$  to form acyclic structures located in deep potential energy wells of about  $310\text{--}410 \text{ kJ mol}^{-1}$ . The latter were found to decompose via atomic hydrogen loss thru relatively tight exit transition states located  $10\text{--}14 \text{ kJ mol}^{-1}$  above the separated reactants.

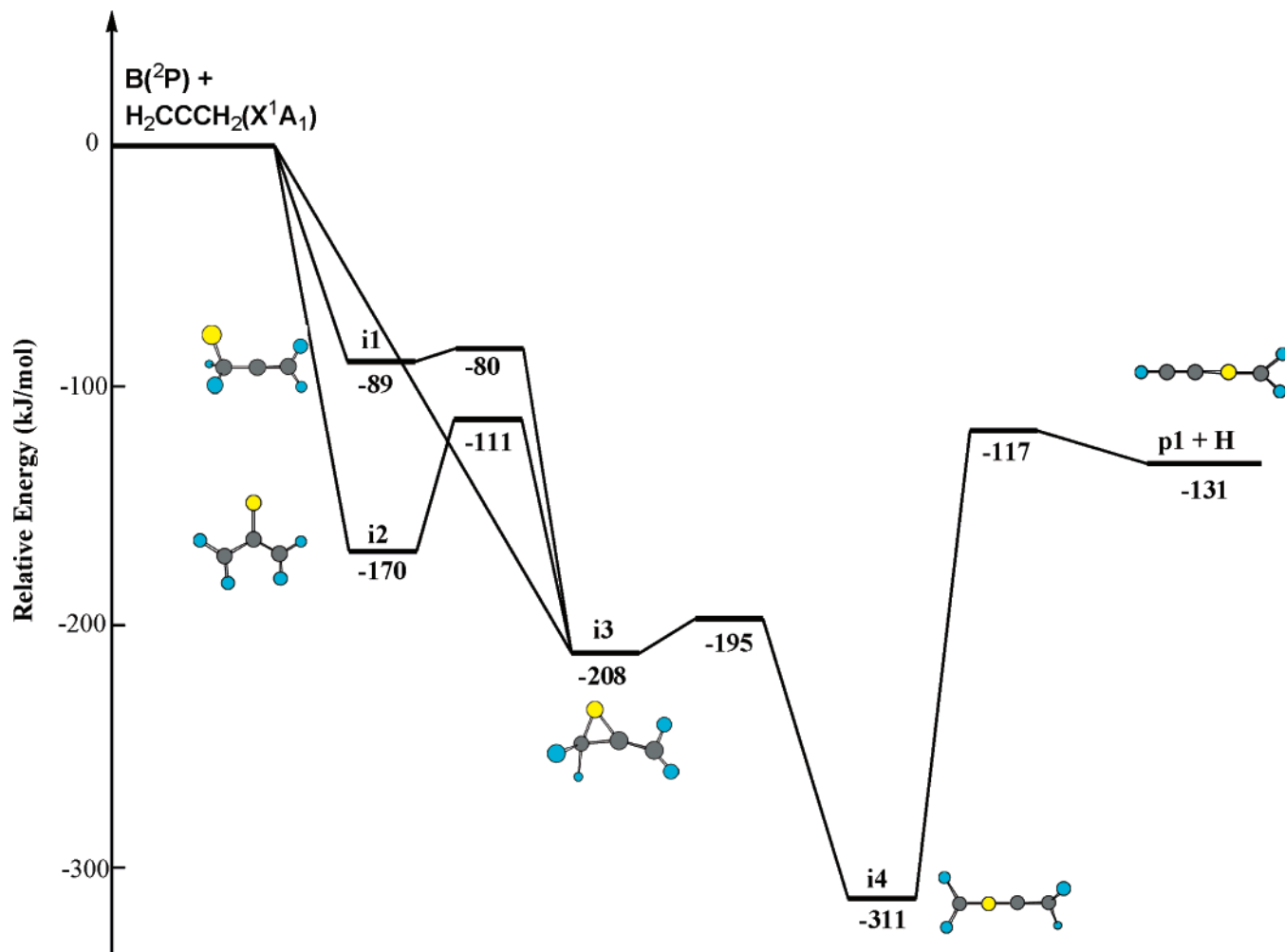


**Figure 5.** Schematic representation of the relevant points of the potential energy surface involved in the reaction of  $B(^2P_j)$  with allene ( $H_2CCCH_2(X^1A_1)$ ) leading to the **p1** isomer of  $^{11}BC_3H_3$  (key: blue, hydrogen; black, carbon; yellow, boron).

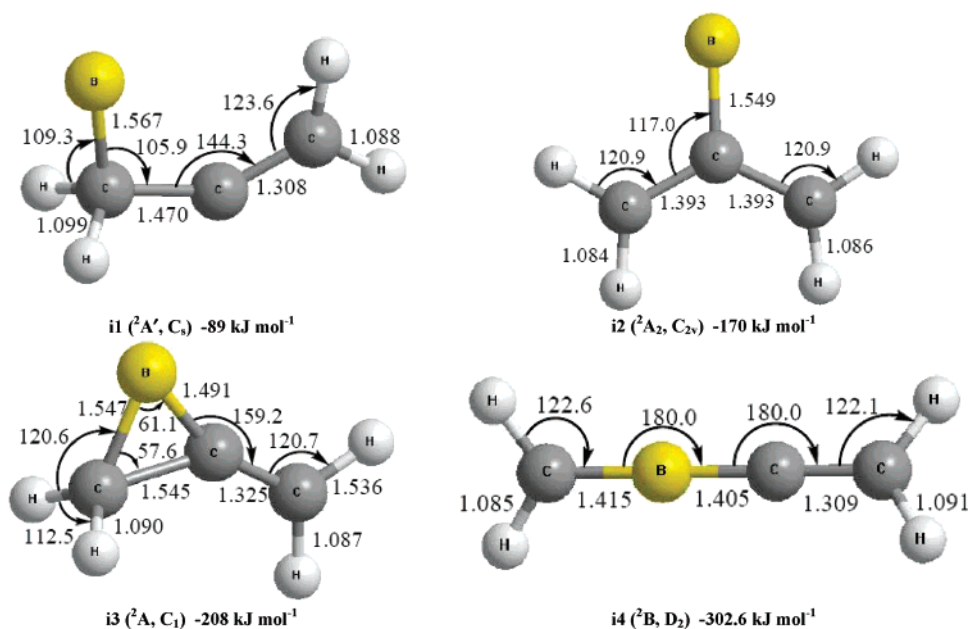


**Figure 6.** Structures of various  $^{11}BC_3H_4$  intermediates. Bond angles and lengths are given in degrees and angstroms, respectively. Electronic ground states and point groups are given in parentheses (key: yellow, boron; gray, hydrogen; black, carbon).

The related boron–methylacetylene reaction is also initiated by an addition of the boron atom to the unsaturated bond. By conducting an experiment with methylacetylene- $d_3$  ( $CD_3CCH$ ), the authors could verify the existence of two microchannels

leading to distinct  $C_{2v}$  symmetric, closed shell isotopomers of **p2**:  $D_2C=C=C=C-B-D$  and  $D_2C=C=C=B-H$ .<sup>44</sup> Summarized, the investigation of the  $^{11}B/C_3H_4$  system demonstrated the formation of two distinct structural product isomers **p1** (H–

$C\equiv C-B=CH_2$ ) (allene reaction) and **p2** ( $H_2C=C=C=B-H$ ) (methylacetylene reaction). This is in contrast to the reactions of ground state carbon atoms,  $C(^3P_1)$ , with allene and methylacetylene, where under single collision conditions only the  $C_s$  symmetric, resonantly stabilized  $i-C_4H_3$  radical was formed.<sup>38,41</sup> Because in the allene system, the hydrogen atoms are equivalent, it is not feasible to utilize partially deuteration of the reactants as done in the methylacetylene- $d_3$  reaction to elucidate the role of thermodynamically less stable isomers **p2**–**p4** on the reaction dynamics. A comprehensive study of the global  $BC_3H_4$  PES combined with RRKM calculations is currently underway.

**Acknowledgment.** This work was supported by the Air Force Office of Scientific Research (AFOSR; W911NF-05-1-0448). We thank Ed Kawamura (University of Hawaii, Department of Chemistry) for his electrical work. A.H.H.C. thanks the National Center for High Performance Computer in Taiwan for the support of computer resources.

## References and Notes

- Schadow, K. C.; Wilson, K. J.; Gutmark, E.; Smith, R. A. Effect of gaseous fuel mixing on boron combustion in ducted rocket with side dump. In *Combust. Boron-Based Solid Propellants Solid Fuels*; 1993; pp 402.
- Ulas, A.; Kuo, K. K.; Gotzmer, C. *Combust. Flame* **2001**, *127*, 1935.
- Mota, J. M.; Abenojar, J.; Martinez, M. A.; Velasco, F.; Criado, A. *J. Solid State Chem.* **2004**, *177*, 619.
- Jin, H. W.; Li, Q. S. *Phys. Chem. Chem. Phys.* **2003**, *5*, 1110.
- Liu, C. H. *Mater. Lett.* **2001**, *49*, 308.
- Loktev, V. M.; Pogorelov, Y. G. *Dopovidi Natsional'noi Akademii Nauk Ukraini* **2005**, *72*.
- Rada, S.; Dumitrescu, I. S. *Stud. Univ. Babeş-Bolyai, Chem.* **2005**, *50*, 297.
- Si, M. S.; Xue, D. S. *Europhys. Lett.* **2006**, *76*, 664.
- Xu, T. T.; Nicholls, A. W.; Ruoff, R. S. *Nano* **2006**, *1*, 55.
- Gertsev, V. V.; Romanov, Y. A. *Khim. Geterotsikl. Soedin.* **1989**, *1483*.
- Ishiyama, T.; Miyaura, N. *Yuki Gosei Kagaku Kyokaiishi* **1999**, *57*, 503.
- Ishiyama, T.; Miyaura, N. *Chem. Record* **2004**, *3*, 271.
- Flores, J. R.; Largo, A. *J. Phys. Chem.* **1992**, *96*, 3015.
- Andrews, L.; Hassanzadeh, P.; Martin, J. M. L.; Taylor, P. R. *AIP Conf. Proc.* **1993**, *288*, 137.
- Andrews, L.; Hassanzadeh, P.; Martin, J. M. L.; Taylor, P. R. *J. Phys. Chem.* **1993**, *97*, 5839.
- Martin, J. M. L.; Taylor, P. R.; Hassanzadeh, P.; Andrews, L. *J. Am. Chem. Soc.* **1993**, *115*, 2510.
- Andrews, L.; Lanzisera, D. V.; Hassanzadeh, P.; Hannachi, Y. *J. Phys. Chem. A* **1998**, *102*, 3259.
- Galland, N.; Hannachi, Y.; Lanzisera, D. V.; Andrews, L. *Chem. Phys.* **1998**, *230*, 143.
- Geppert, W. D.; Goulay, F.; Naulin, C.; Costes, M.; Canosa, A.; Le, Picard, S. D.; Rowe, B. R. *Phys. Chem. Chem. Phys.* **2004**, *6*, 566.
- Balucani, N.; Asvany, O.; Lee, Y. T.; Kaiser, R. I.; Galland, N.; Hannachi, Y. *J. Am. Chem. Soc.* **2000**, *122*, 11234.
- Balucani, N.; Asvany, O.; Lee, Y. T.; Kaiser, R. I.; Galland, N.; Rayez, M. T.; Hannachi, Y. *J. Comput. Chem.* **2001**, *22*, 1359.
- Kaiser, R. I.; Bettinger, H. F. *Angew. Chem. Int. Ed.* **2002**, *41*, 2350.
- Sillars, D.; Kaiser, R. I.; Galland, N.; Hannachi, Y. *J. Phys. Chem. A* **2003**, *107*, 5149.
- Kaiser, R. I.; Balucani, N.; Galland, N.; Caralp, F.; Rayez, M. T.; Hannachi, Y. *Phys. Chem. Chem. Phys.* **2004**, *6*, 2205.
- Bettinger, H. F.; Kaiser, R. I. *J. Phys. Chem. A* **2004**, *108*, 4576.
- Lin, M. C.; Shortridge, R. G.; Umstead, M. E. *Chem. Phys. Lett.* **1976**, *37*, 279.
- Tsuji, M.; Aizawa, M.; Oda, E.; Nishimura, Y. *J. Mass Spectrom. Soc. Jpn.* **1997**, *45*, 493.
- Farrell, J. T.; Taatjes, C. A. *J. Phys. Chem. A* **1998**, *102*, 4846.
- Hoobler, R. J.; Leone, S. R. *J. Phys. Chem. A* **1999**, *103*, 1342.
- Mebel, A. M.; Kaiser, R. I.; Lee, Y. T. *J. Am. Chem. Soc.* **2000**, *122*, 1776.
- Mebel, A. M.; Kisiov, V. V.; Kaiser, R. I. *J. Chem. Phys.* **2006**, *125*, 133113/1.
- Shagun, V. A.; Tarasova, O. A.; Trofimov, B. A. *Russ. J. Org. Chem.* **2006**, *42*, 1039.
- Farrell, J. T.; Taatjes, C. A. *J. Phys. Chem. A* **2002**, *106*, 11992.
- Balucani, N.; Asvany, O.; Huang, L. C. L.; Lee, Y. T.; Kaiser, R. I.; Osamura, Y.; Bettinger, H. F. *Astrophys. J.* **2000**, *545*, 892.
- Balucani, N.; Asvany, O.; Kaiser, R. I.; Osamura, Y. *J. Phys. Chem. A* **2002**, *106*, 4301.
- Guo, Y.; Gu, X.; Zhang, F.; Mebel, A. M.; Kaiser, R. I. *J. Phys. Chem. A* **2006**, *110*, 10699.
- Balucani, N.; Asvany, O.; Osamura, Y.; Huang, L. C. L.; Lee, Y. T.; Kaiser, R. I. *Planet. Space Sci.* **2000**, *48*, 447.
- Kaiser, R. I.; Mebel, A. M.; Chang, A. H. H.; Lin, S. H.; Lee, Y. T. *J. Chem. Phys.* **1999**, *110*, 10330.
- Schmoltner, A. M.; Huang, S. Y.; Brudzynski, R. J.; Chu, P. M.; Lee, Y. T. *J. Chem. Phys.* **1993**, *99*, 1644.
- Kaiser, R. I.; Balucani, N. *Acc. Chem. Res.* **2001**, *34*, 699.
- Kaiser, R. I.; Stranges, D.; Lee, Y. T.; Suits, A. G. *J. Chem. Phys.* **1996**, *105*, 8721.
- Kaiser, R. I.; Le, T. N.; Nguyen, T. L.; Mebel, A. M.; Balucani, N.; Lee, Y. T.; Stahl, F.; Schleyer, P. v. R.; Schaefer, H. F., III. *Faraday Discuss.* **2001**, *119*, 51.
- Guo, Y.; Gu, X.; Balucani, N.; Kaiser, R. I. *J. Phys. Chem. A* **2006**, *110*, 6245.
- Zhang, F.; Kao, C. H.; Chang, A. H. H.; Gu, X.; Guo, Y.; Kaiser, R. I. Submitted to *J. Phys. Chem. A*.
- Gu, X.; Guo, Y.; Kaiser, R. I. *Int. J. Mass Spectrom.* **2005**, *246*, 29.
- Gu, X. B.; Guo, Y.; Chan, H.; Kawamura, E.; Kaiser, R. I. *Rev. Sci. Instrum.* **2005**, *76*, 116103/1.
- Gu, X. B.; Guo, Y.; Kawamura, E.; Kaiser, R. I. *Rev. Sci. Instrum.* **2005**, *76*, 083115/1.
- Gu, X.; Guo, Y.; Kawamura, E.; Kaiser, R. I. *J. Vac. Sci. Technol., A* **2006**, *24*, 505.
- Zhang, F.; Guo, Y.; Gu, X.; Kaiser, R. I. *Chem. Phys. Lett.* **2007**, *440*, 56.
- Vernon, M. Ph.D., University of California, Berkeley, 1981.
- Weiss, M. S. Ph.D., University of California, Berkeley, 1986.
- Zhang, F.; Gu, X.; Kaiser, R. I.; Bettinger, H. Submitted to *Chem. Phys. Lett.*, in press.
- Miller, W. B.; Safron, S. A.; Herschbach, D. R. *Discuss. Faraday Soc.* **1967**, No. 44, 108.
- Becke, A. D. *J. Chem. Phys.* **1993**, *98*, 5648.
- Lee, C.; Yang, W.; Parr, R. G. *Phys. Rev. B: Condens. Matter Mater. Phys.* **1988**, *37*, 785.
- Krishnan, R.; Binkley, J. S.; Seeger, R.; Pople, J. A. *J. Chem. Phys.* **1980**, *72*, 650.
- McLean, A. D.; Chandler, G. S. *J. Chem. Phys.* **1980**, *72*, 5639.
- Purvis, G. D., III; Bartlett, R. J. *J. Chem. Phys.* **1982**, *76*, 1910.
- Hampel, C.; Peterson, K. A.; Werner, H. J. *Chem. Phys. Lett.* **1992**, *192*, 332.
- Knowles, P. J.; Hampel, C.; Werner, H. J. *J. Chem. Phys.* **1993**, *99*, 5219.
- Deegan, M. J. O.; Knowles, P. J. *Chem. Phys. Lett.* **1994**, *227*, 321.
- Frisch, M. J.; Trucks, G. W.; Schlegel, H. B.; Scuseria, G. E.; Robb, M. A.; Cheeseman, J. R.; Zakrzewski, V. G.; Montgomery, J. A., Jr.; Stratmann, R. E.; Burant, J. C.; Dapprich, S.; Millam, J. M.; Daniels, A. D.; Kudin, K. N.; Strain, M. C.; Farkas, O.; Tomasi, J.; Barone, V.; Cossi, M.; Cammi, R.; Mennucci, B.; Pomelli, C.; Adamo, C.; Clifford, S.; Ochterski, J.; Petersson, G. A.; Ayala, P. Y.; Cui, Q.; Morokuma, K.; Malick, D. K.; Rabuck, A. D.; Raghavachari, K.; Foresman, J. B.; Cioslowski, J.; Ortiz, J. V.; Baboul, A. G.; Stefanov, B. B.; G. Liu, A. L.; Piskorz, P.; Komaromi, I.; Gomperts, R.; Martin, R. L.; Fox, D. J.; Keith, T.; Al-Laham, M. A.; Peng, C. Y.; Nanayakkara, A.; Gonzalez, C.; Challacombe, M.; Gill, P. M. W.; Johnson, B. G.; Chen, W.; Wong, M. W.; Andres, J. L.; Head-Gordon, M.; Replogle, E. S.; Pople, J. A. *Gaussian 98*, revision A5; Gaussian, Inc.: Pittsburgh, PA, 1998.
- Frisch, M. J.; Trucks, G. W.; Schlegel, H. B.; Scuseria, G. E.; Robb, M. A.; Cheeseman, J. R.; Montgomery, J. A., Jr.; Vreven, K. T.; Kudin, N.; Burant, J. C.; Millam, J. M.; Iyengar, S. S.; Tomasi, J.; Barone, V.; Mennucci, B.; Cossi, M.; Scalmani, G.; Rega, N.; Petersson, G. A.; Nakatsuji, H.; Hada, M.; Ehara, M.; Toyota, K.; Fukuda, R.; Hasegawa, J.; Ishida, M.; Nakajima, T.; Honda, Y.; Kitao, O.; Nakai, H.; Klene, M.; Li, X.; Knox, J. E.; Hratchian, H. P.; Cross, J. B.; Bakken, V.; Adamo, C.; Jaramillo, J.; Gomperts, R.; Stratmann, R. E.; Yazyev, O.; Austin, A. J.; Cammi, R.; Pomelli, C.; Ochterski, J. W.; Ayala, P. Y.; Morokuma, K.; Voth, G. A.; Salvador, P.; Dannenberg, J. J.; Zakrzewski, V. G.; Dapprich, S.; Daniels, A. D.; Strain, M. C.; Farkas, O.; Malick, D. K.; Rabuck, A. D.; Raghavachari, K.; Foresman, J. B.; Ortiz, J. V.; Cui, Q.; Baboul, A. G.; Clifford, S.; Cioslowski, J.; Stefanov, B. B.; Liu, G.; Liashenko, A.; Piskorz, P.; Komaromi, I.; Martin, R. L.; Fox, D. J.; Keith, T.; Al-Laham, M. A.; Peng, C. Y.; Nanayakkara, A.; Challacombe, M.; Gill, P. M. W.; Johnson, B.; Chen, W.; Wong, M. W.; Gonzalez, C.; Pople, J. A. *Gaussian 03*, revision C.02; Gaussian, Inc.: Wallingford, CT, 2004.
- Bentz, T.; Giri, B. R.; Hippler, H.; Olzmann, M.; Striebel, F.; Szoeri, M. *J. Phys. Chem. A* **2007**, *111*, 3812.